Electron capture β decay of ^{7}Be located inside and outside the C_{36} fullerene

E. V. Tkalya,[1,*] A. V. Avdeenkov,[1,2] A. V. Bibikov,[1] I. V. Bodrenko,[1,3] and A. V. Nikolaev[1,4]

[1]*Skobeltsyn Institute of Nuclear Physics, Lomonosov Moscow State University, Leninskie gory, RU-119234 Moscow, Russia*

[2]*National Institute for Theoretical Physics, Stellenbosch Institute of Advanced Study, Private Bag X1, Matieland 7602, South Africa*

[3]*National Nanotechnology Laboratory (NNL), Istituto Nanoscienze–CNR, Via per Arnesano 16, I-73100 Lecce, Italy*

[4]*Institute of Physical Chemistry of RAS, Leninskii pr. 31, RU-117915 Moscow, Russia*

(Received 26 January 2012; revised manuscript received 25 June 2012; published 11 July 2012)

Equilibrium positions of the ^{7}Be atom both inside and outside the C_{36} fullerene are found and the electron density at the ^{7}Be nucleus, $\rho(0)$, for these positions are calculated using a high-accuracy *ab initio* post-Hartree-Fock method. If ^{7}Be is located outside the C_{36} cage the electron density at the ^{7}Be nucleus practically coincides with $\rho(0)$ of a single ^{7}Be atom. In the encapsulated ^{7}Be@C_{36} case $\rho(0)$ is found to lie close to the electron density $\rho(0)$ of the $^7Be^{2+}$ ion with the unoccupied $2s$ electron shell, which results in the smallest value among all known ^{7}Be-based compounds where the influence of chemical environment on the probability of electron capture by ^{7}Be has been investigated. Consequently, the ^{7}Be half-life in the ^{7}Be@C_{36} molecular complex is expected to be the largest.

DOI: 10.1103/PhysRevC.86.014608 PACS number(s): 21.10.Tg, 23.40.Hc, 27.20.+n, 36.40.Cg

I. INTRODUCTION

Electron capture (or "K-capture") is a well-known process whereby a nucleus of charge Z absorbs an electron from an atomic shell and through the nuclear reaction $p + e^- \rightarrow n + \nu_e$ transforms to a nucleus of charge $Z - 1$. The necessary condition for the reaction is a nonzero value of the electron wave function (WF) amplitude at the nucleus. Since electronic states of an atom or a molecule depend on their chemical environment and differ from the states of isolated atoms or molecules, the probability of electron capture also shows such a dependence.

^{7}Be is a very convenient nucleus to study the influence of chemical environment on electron capture. The electron atomic configuration of Be is $(1s)^2(2s)^2$. The WF amplitude of s states is maximal at the nucleus. The contribution of the valence $2s$ electrons to the electron density at the ^{7}Be nucleus, $\rho(0)$, is relatively large and amounts to 3.2%. The $2s$ electrons are delocalized in some Be-based compounds, creating a metallic bond (for example, in metallic Be) but they can also participate in covalent or ionic bonding in others, thereby forming the mechanism of the influence of chemical environment on the probability of ^{7}Be nuclear decay.

In the present study we report on the results of our calculations for the ^{7}Be nucleus when ^{7}Be is encapsulated in C_{36} (^{7}Be@C_{36}) and when ^{7}Be is outside the fullerene cage (^{7}Be-C_{36}) and demonstrate the effect of chemical environment on nuclear properties. First, according to our investigations ^{7}Be@C_{36} shows the longest half-life of ^{7}Be because of the effect of chemical environment. [It is worth noting that the shortest half-life of ^{7}Be is realized when ^{7}Be is encapsulated in another fullerene—C_{60} (see below).] Second, the calculations give for the compound ^{7}Be-C_{36} a half-life for ^{7}Be that practically coincides with the half-life of the nucleus ^{7}Be in the free atom. The predicted effects reflect the crucial role of physical and chemical interactions in ^{7}Be@C_{36} and ^{7}Be-C_{36} and can be checked experimentally.

The paper is organized as follows. In Sec. II we review available experimental data on the ^{7}Be half-life in various compounds. Then, in Sec. III we briefly describe the technical aspects of our calculational method and the choice of basis functions which allow us to extract the electron density at ^{7}Be, $\rho(0)$. In Sec. IV we study the equilibrium positions of ^{7}Be both inside and outside the fullerene cage, present calculations of $\rho(0)$, and discuss the results of our findings. Finally, our main conclusions are given in Sec. V.

II. REVIEW OF EXPERIMENTAL DATA

The first measurements of the nuclear decay constant of ^{7}Be dates back to the middle of the last century [1–5]. Nowadays the number of reported data on the half-life and decay constant of ^{7}Be amounts to dozens.

These data can be distinguished according to the type of binding between Be and its chemical environment. First of all, it depends on the type of chemical bond (i.e., ionic, covalent, etc.). Experiments with ^{7}Be were performed for the following compounds: ^{7}BeO [2,4–7], $^7BeF_2$ [4–6], $^7BeBr_2$ [6], $^7Be(OH)_2$ [7], $^7Be^{2+}(OH_2)_4$ [6,7], $^7Be_4O(CH_3COO)_6$ [6], and $^7Be(C_5H_5)$ [6]. Second, ^{7}Be was inserted into various metals: Al [8,9], Au [10–13], Cu [9,14], Pd [15], Ta [11,15,16], W [15], and Zr [15], as well as the beryllium metal itself [2,4–6,10,12,17]. Third, ^{7}Be was implanted in nonmetallic compounds: sapphire (Al_2O_3) [9,10], lithium fluoride (LiF) [18], graphite [11], polyvinyl chloride [9], boron nitride [11], and fullerene C_{60} [13,17,19]. Finally, there are data for various pressures or temperatures: (a) on ^{7}BeO [20] at elevated pressure up to 270 kbars and on $^7Be(OH)_2$ [21] at 400 kbars and (b) on ^{7}Be@C_{60} at temperature as low as 5 K [17]. Also, half-life measurements have been performed for ^{7}Be in Cu at 12.5 K [14] and decay constant measurements have been made for ^{7}Be in Pd, In, and Li_2O at 293 and 12 K [22].

*tkalya@srd.sinp.msu.ru

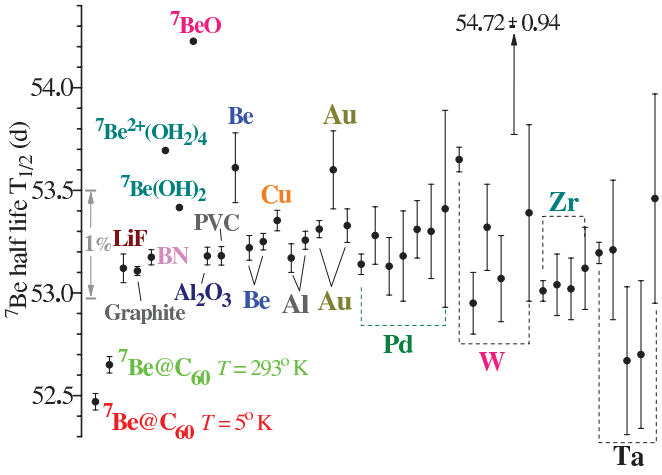

FIG. 1. (Color online) Experimental half-lives of the ^{7}Be nucleus in various chemical environments. The label "Be" stands for metallic ^{7}Be, labels "Cu", "LiF," and others stand for crystals of Cu, LiF, etc. with implanted ^{7}Be.

There are only a few theoretical works on the problem in the literature. It is worth mentioning the fundamental review [23] on electron capture in nuclei and studies [24–29] where electron capture phenomena are explained more or less satisfactory. Theoretical approaches applied to calculations of ^{7}Be are discussed in detail in Ref. [29].

The ^{7}Be half-life in some compounds and the relative difference of ^{7}Be decay constants for various pairs of compounds from the cited works are summarized in Fig. 1 and Fig. 2, respectively. They give a clear picture of the influence of the chemical environment on the probability of electron capture by ^{7}Be. In most cases the experimental accuracy is less than 1%. However, there are apparently contradicting results (for example, half-life data for BeO and metallic Be in Fig. 1 and $\Delta\lambda/\lambda$ for the same pair in Fig. 2).

Inspection of Fig. 1 shows that the smallest half-life for ^{7}Be is observed in Be@C_{60}. The largest half-life, which is 53.69 d, is found in $^7Be^{2+}(OH_2)_4$ [7]. However, this singular

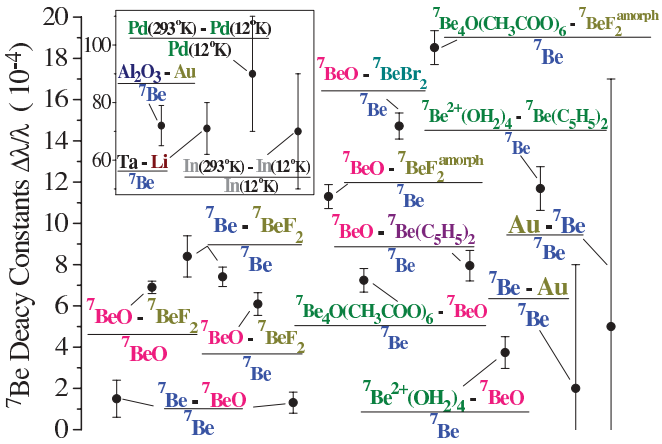

FIG. 2. (Color online) Experimental relative differences of ^{7}Be decay constants, i.e., $(\lambda_1 - \lambda_2)/\lambda_3$, in various chemical environments. The labels are as in the caption of Fig. 1. No change of decay constant on cooling of Li_2O was found: $\Delta\lambda/\lambda = 0.2 \pm 0.3\%$ [22].

measurement requires an additional confirmation. As for the two highest points marked as "BeO" ($T_{1/2} = 54.23$ d [7]) and "W" ($T_{1/2} = 54.72$ d [15]) in Fig. 1, they are inconsistent with other experimental data and most likely are erroneous. Also, the ^{7}Be half-life in metallic beryllium (point "Be" in Fig. 1 with $T_{1/2} = 53.61$ d [5]) and in gold ("Au" in Fig. 1 with $T_{1/2} = 54.23$ d [7]) and a very high value of the half-life in tungsten ("W", $T_{1/2} = 53.65$ [15]) are very different from the other measurements. Therefore, by now it can be safely stated that the largest ^{7}Be half-life in a medium does not exceed 53.5 d. Anticipating our results for ^{7}Be@C_{36} we mention here that the predicted considerable slowdown of the decay of ^{7}Be in this complex can be of interest to experimental verification.

Finally, we notice that the absence of reliable data on the ^{7}Be half-life for a single Be atom also hinders our consideration. Although such an experiment is complicated it would directly relate the calculated results with the experiment because the electron density in the Be atom can be calculated with a very high precision. Nowadays as the reference point for the ^{7}Be half-life, instead of atomic data, the half-life in metallic ^{7}Be is used, but there are many experimental and computational complexities which are associated with that system and lead to relatively high uncertainties and inaccuracies.

III. CALCULATION PROCEDURE

For the present study we assume that the C_{36} fullerene has the highest allowed molecular symmetry, which is D_{6h} with the six-fold rotation axis and the perpendicular to its mirror plane (see also Sec. IV below). According to Ref. [30] this structure has the lowest ground-state energy in the C_{36} family. We have also confirmed this conclusion by comparing the ground-state energies of 15 main isomers of C_{36}. The isomers were calculated within the Hartree-Fock method with the 6-31G** basis and electronic correlations accounted for in the second order of the Møller-Plesset perturbation scheme (MP2) [31]. The final geometry of C_{36} has been obtained by optimizing six independent parameters of the D_{6h} structure.

For calculations of the electron density $\rho(r)$ we follow the method of Ref. [29], which has been applied earlier to extract the electron density at the ^{7}Be nucleus in the ^{7}Be@C_{60} complex. In brief, an original implementation of the Hartree-Fock method described in Ref. [32] is employed. For calculations of the energy of electron orbitals the electron correlations are included within the MP2 approach or within a more refined configuration interaction (CI) method tested in Ref. [33]. The program suite includes codes for geometry optimization and optimal basis selection. Special care has been undertaken to accelerate the computation process while keeping a high precision for energy ($\sim 10^{-3}$ eV for the van der Waals interaction) and density. The suite has been proven advantageous when it was applied to a number of computational problems. In particular, it was used in ^{7}Be@C_{60} [29] to determine the electron density at ^{7}Be and to study the molecular term energy spectrum of the neutral C_{60} fullerene [33] (CI approach).

Precise calculation of the electron density at the nucleus with the Gaussian-type basis constitutes a well-known problem

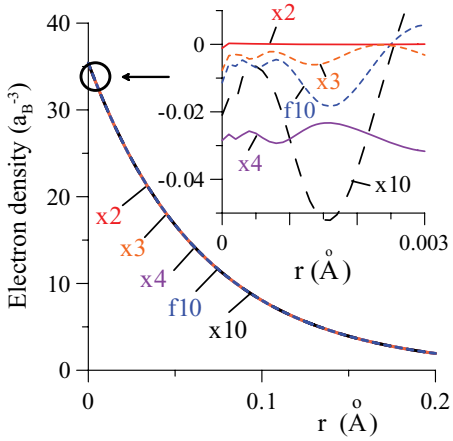

FIG. 3. (Color online) The electron density of the Be atom in the vicinity of its nucleus with the cc-pVTZ basis supplemented by various sets of narrow Be s functions (see text for details). The inset shows the residuals after the linear dependence of the best set (tz_Be_x2) is subtracted from $\rho(r)$.

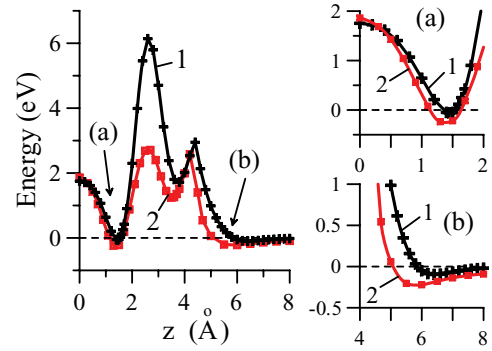

FIG. 4. (Color online) The ground-state energy of the complex of ^{7}Be and C_{36} as a function of the position of ^{7}Be on the z axis. Plot 1 corresponds to the fixed geometry of C_{36}; plot 2 corresponds to the optimized geometry (see text for details). (a) is the minimum when ^{7}Be is encapsulated in C_{36} (^{7}Be@C_{36}); (b) is the van der Waals minimum when ^{7}Be is located outside C_{36}.

[31]. The s-electron states are better reproduced by Slater-type functions which have finite slopes at $r = 0$ whereas the Gaussian function has a zero slope at $r = 0$. Therefore, more Gaussian functions are required for the adequate description as r approaches the nucleus. In the present study the problem has been solved by supplementing the standard Dunning basis set cc-pVTZ [34] by narrow s functions $f_i = \exp(-\lambda_i r^2/2)$ centered at the beryllium site. Four supplemental sets have been used: tz_Be_x10, tz_Be_x4, tz_Be_x3, and tz_Be_x2. Within each of the sets the Gaussian orbital exponents λ_i of the functions f_i form a geometric progression starting with $\lambda_1 \simeq 0.1$ and ending with $\lambda_{\max} \simeq 10^8$. In the four supplemental sets the progression ratio q is 10, 4, 3, and 2 (as also indicated in the set label), and the number of functions is 7, 18, 20, and 34, respectively, so that the best set is tz_Be_x2. In addition we have used the basis set tz_Be_f10, which has the Gaussian primitives of tz_Be_x10 but no contraction is imposed. The results for the Be atom are depicted in Fig. 3 for $0 \leqslant r \leqslant 0.2$ Å. Notice that $\lambda_{\max} \simeq 10^8$ allows us to correctly calculate the Be electron density down to $r \simeq 10^{-4}$ Å. In the scale of Fig. 3 the curves corresponding to different supplemental sets are practically indistinguishable. Therefore, we exclude the linear dependence of the best set from the curves and plot the residuals in the smaller range $0 \leqslant r \leqslant 0.003$ Å as shown in the inset of Fig. 3. It is clear that the maximal density deviation lies within 0.03 a_B^3, which should be taken as our calculation accuracy for the electron density at the ^{7}Be nucleus. This precision is very high and is as good as the experimental one.

As we have mentioned earlier the calculations have been performed by taking into account the effect of electron correlations by including the MP2 contribution to the ground-state energy [31]. For the most important points in the vicinity of minima and maxima of the potential energy curve in Fig. 4 we have used the CI procedure with single and double excitations (SDCI) of the reference Hartree-Fock determinant in the active space including the 4 highest occupied molecular orbitals and 50 lowest unoccupied molecular orbitals. It has turned out that the corrections are small (the maximal deviation being 0.25 eV) and does not influence the characteristic energy profiles. A thorough discussion of Fig. 4 is given in the next section.

IV. RESULTS OF NUMERICAL CALCULATIONS

A. Energy minima and equilibrium geometries

We start our calculations by finding the optimal equilibrium positions of ^{7}Be with respect to the C_{36} fullerene. The D_{6h} isomer of C_{36} has a single six-fold axis of symmetry and if the ^{7}Be nucleus is located on the axis the six-fold rotation symmetry C_6 is conserved while the σ_h reflection plane is not. If we chose the C_6 axis as the z axis with the origin at the center of the fullerene, then the position of the ^{7}Be nucleus on it is completely defined by its z coordinate, z_{Be}.

First we have calculated the ground-state energy of the molecular system as a function of z_{Be}, keeping the molecular geometry of C_{36} unchanged, and obtained the dependence shown in Fig. 4 as plot 1. We clearly see the appearance of two minima (a) and (b) at $z_{Be} \sim 1.5$ Å and $z_{Be} \sim 6$ Å. The first minimum (1.5 Å) corresponds to the beryllium atom encapsulated in C_{36}, i.e., ^{7}Be@C_{36}, and is caused by the Hartree-Fock binding, while the second one (6 Å) with ^{7}Be located outside the fullerene is due to the electron correlation (MP2 or CI) energy contribution driven by the van der Waals forces (see the two panels on the right-hand side of Fig. 4). The charge states of the ^{7}Be atom in the two minima are also different. At small z_{Be} two valence $2s$ electrons of ^{7}Be are mainly transferred to the fullerene cage while at large z_{Be} ^{7}Be becomes neutral (an effect which we will discuss in detail below). In the middle region we find two maxima at $z_{Be} \sim 2.6$ Å and $z_{Be} \sim 4.5$ Å. The 2.6-Å maximum with a 6-eV height develops when ^{7}Be passes through the hexagonal facet of C_{36}. It is driven by strong repulsion between Be and the C_6 carbon hexagon. The other maximum at 4.5 Å appears when ^{7}Be is located at 1.9 Å from the edge hexagon. We attribute this maximum to the effect of charge transfer from the fullerene back to the beryllium atom, which as a result

becomes neutral. Finally, between the two maxima we find a local metastable minimum at $z \sim 3.7$ Å.

Next, we consider the effect of the relaxation of the carbon cage of C_{36}. Since the fullerene is a large molecular system we limit ourselves to the optimization of only 12 carbon atoms nearest to the z axis and belonging to that half of the C_{36} fullerene which has ^{7}Be in it. (Six out of 12 carbon atoms belong to the facet hexagon which crosses the z axis and the other six form a second carbon shell close to the hexagon.) The optimization has only four independent parameters and keeps the C_{6v} symmetry of the molecular complex. The results of calculations for that case are presented in Fig. 4 as plot 2. Notice that the main effect is a substantial, down to 3 eV, reduction of the potential barrier at $z_{Be} \sim 2.6$ Å, which is facilitated by the displacement of the 12 carbon atoms. It is worth noticing that this value is in agreement with the characteristic potential barrier for the formation of endohedral fullerenes [35]. Another important effect is the deepening of the van der Waals minimum, which shifts to a smaller value of $z = 5.7$ Å. The ^{7}Be@C_{36} minimum, the metastable local minimum, and the second barrier also shift to smaller z_{Be}, 1.4, 3.5, and 4.2 Å, respectively. The 4.2-Å barrier becomes lower but the effect is much less pronounced in comparison with the 2.6-Å barrier. It is instructive to analyze the effect of electron correlations on the potential curve. The MP2 contribution tends to elevate the 1.4-Å minimum (^{7}Be@C_{36}) and to lower the 5.7-Å van der Waals minimum (^{7}Be-C_{36}). The CI corrections also follow this trend. In order to study the effect more accurately we have performed a few calculations allowing the full fullerene cage relaxation within the C_{6v} symmetry, which implies optimization over 12 independent parameters. These precise calculations confirmed our results and place the van der Waals minimum at ~ 0.03 eV below the ^{7}Be@C_{36} minimum.

Finally, we have studied the potential energy of the ^{7}Be@C_{36} molecular complex when ^{7}Be is shifted off the z axis while the C_{36} geometry is frozen out. Our calculations show that a slightly better binding is found when ^{7}Be is moved from the z axis toward the center of one of the six pentagons (see left inset in Fig. 5). The z coordinate of ^{7}Be in that case is 1.1 Å, and the distance from the fullerene wall remains almost the same as before. (In fact, this position of the Be atom also corresponds to the positions of some energy minima when the geometry "optimization" of the molecule is allowed; see Sec. IV C.) However, the overall energy gain for the off-z-axis position is small and is not so important for us because the density at the ^{7}Be nucleus, $\rho(0)$, remains practically the same as for the on-z-axis position (see below). The same consideration applies to the van der Waals minimum with ^{7}Be located outside C_{36}. Here a slightly better energy position is found when ^{7}Be moved away from the z axis, as shown in the right inset of Fig. 5. However, the energy gain is insignificant while the distance from the center of the fullerene and the electron density at the ^{7}Be nucleus remain the same within the computation accuracy. Therefore, in the following we consider the situation when ^{7}Be is located on the z axis.

B. Electron density at the ^{7}Be nucleus

The results of the calculation of the electron density at the ^{7}Be nucleus are summarized in Fig. 5. For the ^{7}Be atom located

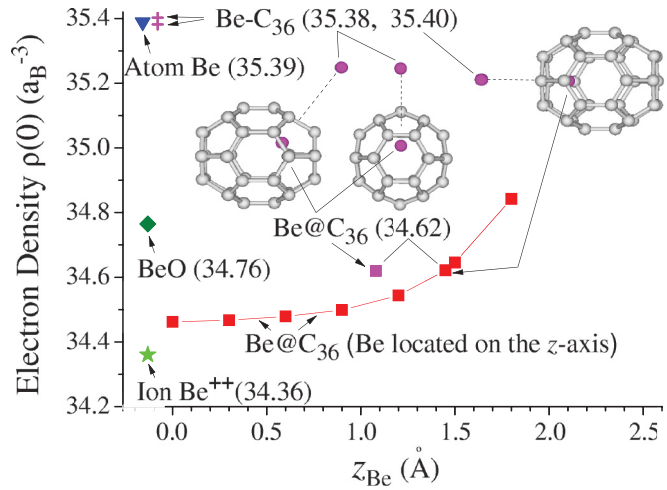

FIG. 5. (Color online) Calculated electron density at the ^{7}Be nucleus when ^{7}Be is encapsulated in C_{36} (^{7}Be@C_{36}) and when ^{7}Be is located outside the fullerene (^{7}Be-C_{36}) (see details in the text). For comparison, electron densities in other compounds are shown. Some of possible equilibrium positions of the Be atom off of the z axis and on the z axis are shown in the insets.

in its possible energy minimums inside the C_{36} fullerene, i.e., for ^{7}Be@C_{36}, we obtain the same value of $\rho(0) = 34.62\ a_B^{-3}$ whether ^{7}Be is located off of the z axis or on the z axis. Notice that this value for the C_{60} fullerene (^{7}Be@C_{60}) is $\rho(0) = 35.48\ a_B^{-3}$ [29]. Since both calculations have been carried out by the same program suite [32] and within the same computational conditions and accuracy we can use these data to estimate the half-life for ^{7}Be encapsulated in C_{36}. The experimental values of the half-life in the ^{7}Be@C_{60} complex are the following [17]: $T_{1/2} = 52.47$ d at 5 K and $T_{1/2} = 52.65$ d at 293 K. From these data, we get $T_{1/2} = 53.7$–54.0 d for ^{7}Be@C_{36}. The half-life of ^{7}Be in C_{36} is 2.5% larger than in C_{60}.

Thus, $\rho(0)$ for ^{7}Be@C_{60} is situated between the values for ^{7}BeO where the valency of Be is two and $^7Be^{2+}$ where the $2s$-electron shell is empty. Therefore, the electron density at ^{7}Be in ^{7}Be@C_{36} is the lowest and the half-life is the largest in comparison with other compounds where the influence of chemical environment on the probability of K-capture has been studied.

If ^{7}Be is encapsulated in C_{36} the electron density at the nucleus, $\rho(0)$, increases with z_{Be}, as shown in Fig. 5. However, $\rho(0)$ drops at $z_{Be} = 3.5$ Å (a local metastable minimum) down to $34.72\ a_B^{-3}$, which is also close to the value of ^{7}BeO. Then $\rho(0)$ rises to $35.38\ a_B^{-3}$ in the van der Waals minimum where it virtually coincides with $\rho(0)$ for the neutral beryllium atom.

C. Influence of the C_{36} deformation on $\rho(0)$

In principle, the determination of the optimum position of ^{7}Be within the fullerene and the calculation of the electron density at the ^{7}Be nucleus, $\rho(0)$, require the full optimization of the ^{7}Be@C_{36} complex. However, the total number of parameters for the ^{7}Be@C_{36} molecule containing 37 atoms is $37 \times 3 - (3 + 3) = 105$ (where here six degrees of freedom are subtracted because they account for translations and

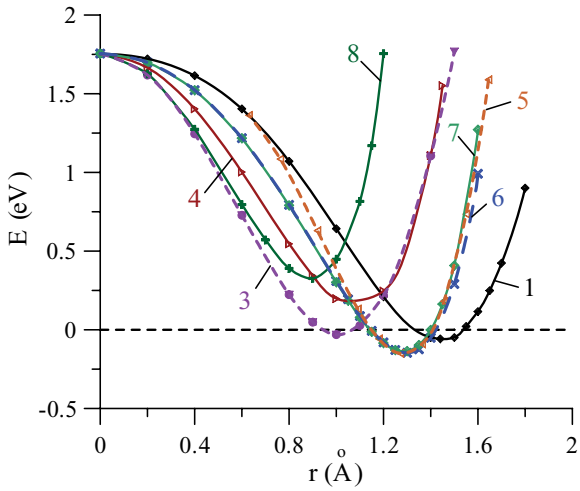

FIG. 6. (Color online) The ground-state energy of the ^{7}Be@C_{36} complex as a function of the position of ^{7}Be: (1) on the z symmetry axis in the fixed geometry of the fullerene (curve 1 in Fig. 4), (3) on the axis passing through the center of the side C_6 carbon hexagon and the center of the fullerene perpendicular to the z axis, (4) on the axis passing through the center of the fullerene and the center of the C_5 carbon pentagon, (5) on the axis passing through the center of the C_5 carbon pentagon perpendicular to its plane, (6) on the axis passing through the center of C_{36} and the midpoint of the C–C bond fusing the C_5 carbon pentagon and the C_6 carbon hexagon, (7) on the axis passing through the center of C_{36} and the C atom belonging to the front C_6 carbon hexagon, and (8) on the line connecting the center of C_{36} and a C atom shared by a C_5 carbon pentagon and two C_6 carbon hexagons which form the middle part of the fullerene. The coordinate r is a distance from the center of the fullerene for all cases (1–8). In (5) the coordinate r satisfies the condition $r > r_{\rm int}$, where $r_{\rm int}$ is the intersection of the perpendicular to the C_5 carbon pentagon with the z axis.

rotations of the molecule as a whole). It is clear that such an optimization in the framework of the Hartree-Fock method makes calculations extremely laborious.

On the other hand, the main purpose of this paper is to make a qualitative prediction of the half-life of the ^{7}Be nucleus in the C_{36} fullerene. The half-life is uniquely related to the magnitude of the electron density at the ^{7}Be nucleus. According to results of our calculations shown in Fig. 5, $\rho(0)$ has a relatively weak dependence on the position of the Be atom inside C_{36}. If the beryllium atom is located on the z axis, which is the molecular symmetry axis, the electron density is 34.4–34.8 a_B^{-3}, i.e., between the densities for the Be^{++} ion and for Be in beryllium oxide, BeO. A partial optimization of the ^{7}Be@C_{36} molecule has not changed the situation. The resulting value of $\rho(0) = 34.62\ a_B^{-3}$ lies in the same range.

In addition, to demonstrate a weak dependence of $\rho(0)$ on the position of Be, we have carried out an exhaustive set of various geometry optimizations. First, we have investigated the dependence of the binding energy of the Be atom inside C_{36}, when Be is displaced in different directions (Fig. 6). For each direction of the Be displacement we have found a minimum of energy and computed the electron density $\rho(0)$ of ^{7}Be there. The results (triangles) are represented in Fig. 7. The data are in agreement with our conclusion that the optimization has very

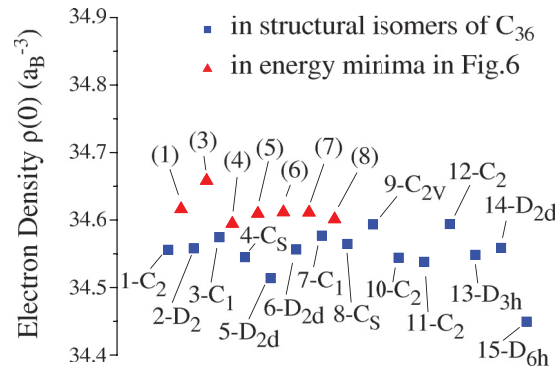

FIG. 7. (Color online) Electron density at the ^{7}Be nucleus located (a) at positions of the energy minima in various directions used in Fig. 6 and (b) at the centers of 15 known structural isomers of C_{36}.

little effect on the magnitude of the electron density $\rho(0)$. For example, for the optimized energy minimum on the z axis we have $\rho(0) = 34.6215\ a_B^{-3}$, while without optimization $\rho(0) = 34.6163\ a_B^{-3}$. Therefore, the difference between the two values amounts to only 0.015%, which is practically negligible.

The space coordinates of Be in the energy minima for cases 5 and 6 almost coincide, and the position of Be for case 7 is also close to that point. This observation explains why binding energies (see Fig. 6) and the electron densities at the Be nucleus (see Fig. 7) are not very different for these cases.

It is important that the optimized position of the Be atom (located off the z axis as shown in the left inset in Fig. 5) lies exactly in the described area, i.e., near the Be positions which give energy minima for cases 5, 6, and 7. Earlier (Sec. IV A) this result was obtained for the fixed geometry of C_{36}. However, as we have already mentioned in Sec. IV A the electron density $\rho(0)$ is not sensitive to the geometry optimization.

Since the geometrical changes of the fullerene cage are very small in the optimization process, we have also investigated the effect of conformation on the density $\rho(0)$. For that purposes we have performed calculations of $\rho(0)$ when the beryllium atom is located at the center of all known conformations of the C_{36} fullerene and plotted the resultant data (squares) in Fig. 7. Variations of $\rho(0)$ in that case are larger than for different minima of Be inside the most stable conformation of C_{36}, but even then the changes are small and do not exceed 0.4%.

Thus, our analysis unambiguously indicates that the calculations with partial geometry optimization give a realistic theoretical estimate of the half-life of the ^{7}Be nucleus in C_{36}.

D. Discussion of the results

The largest half-life of ^{7}Be encapsulated in the C_{36} fullerene seems unexpected in relation to the fact that in the ^{7}Be@C_{60} complex the ^{7}Be half-life is relatively large [17,19]. The detailed mechanism of density variation has been studied in Ref. [29]. There it has been argued that the valence electrons of Be should be considered in the joint effective potential of the ^{7}Be nucleus and the fullerene molecule. It was found that the new wave function of the valence electrons of Be is very sensitive to the finest details of the effective fullerene

TABLE I. Partial contributions $\rho_i(0)$ of the three most important molecular orbitals ($i = 1$–3) to the electron density $\rho(0)$ at the ^{7}Be nucleus when ^{7}Be is encapsulated in C_{36} (^{7}Be@C_{36}) and when Be is located outside C_{36} (^{7}Be-C_{36}). E_i is the Hartree-Fock molecular orbital energy and $\% \equiv [\rho_i(0)/\rho(0)] \times 100\%$.

	^{7}Be@C_{36}			^{7}Be-C_{36}		
i	E_i (eV)	$\rho_i(0)$ (a_B^{-3})	%	E_i (eV)	$\rho_i(0)$ (a_B^{-3})	%
1	− 131.7	34.14	98.62	− 128.5	34.25	96.76
2	− 19.6	0.25	0.71	− 8.2	1.02	2.89
3	− 37.3	0.11	0.33	− 9.1	0.07	0.19

potential and that the increase of the electron density at ^{7}Be located at the center of C_{60} to some extent can be considered as accidental. For example, a substitution of a few carbon atoms with other atoms induces a change in the effective potential of the fullerene cage with a resultant contribution to $\rho(0)$ which can be both positive and negative [29]. The important observation is that in the ^{7}Be@C_{60} molecular complex there is no conventional chemical binding between the ^{7}Be atom and the C_{60} fullerene and therefore the electronic states of ^{7}Be and C_{60} retain their own character.

The situation in ^{7}Be@C_{36} is different. The Be atom is closer to the C_{36} fullerene cage and it is not located at the molecular center. We have selected three molecular orbitals (MOs) giving the largest contributions to the electron density $\rho(0)$ and studied their properties. The results are quoted in Table I. The most important molecular orbital is obviously a slightly modified 1s core electron shell of beryllium. The two next important molecular orbitals are visualized in Figs. 8(a) and 8(b). The second part of Table I refers to the van der Waals binding when the ^{7}Be atom is located outside the C_{36} fullerene and its electronic structure is close to the neutral atom. The two next important molecular orbitals for that case are shown in Figs. 8(c) and 8(d).

It is instructive to compare the situations with ^{7}Be inside and outside the C_{36} cage. In the ^{7}Be@C_{36} case the second and the third important MOs are localized on carbon atoms of the fullerene cage [see Figs. 8(a) and 8(b)]. The chemical bonding is close to ionic with the tails of the functions giving a small contribution to the density at the ^{7}Be nucleus (contributions with $i = 2, 3$ in Table I). The effect is especially pronounced for the $i = 2$ contribution to $\rho(0)$, which in the ^{7}Be@C_{36} case is one quarter as large as that for the van der Waals binding. Notice that in the van der Waals binding the second important MO is spherically symmetric and almost isolated from the fullerene [Fig. 8(c)]. In fact, it is very close to the 2s orbital of the neutral Be atom, as expected from the van der Waals complex.

Therefore, from the point of view of the electron density, $\rho(0)$, in the ^{7}Be@C_{36} molecule ^{7}Be is "oxidized" by C_{36} and the "oxidation" is slightly higher than in ^{7}BeO. The process explains the decrease of $\rho(0)$ and the corresponding increase of the ^{7}Be half-life. In van der Waals binding $\rho(0)$ practically coincides with the value for the neutral ^{7}Be atom. This observation can facilitate the experimental determination of $\rho(0)$ for the ^{7}Be atom, which is necessary for classification of the experimental and theoretical data.

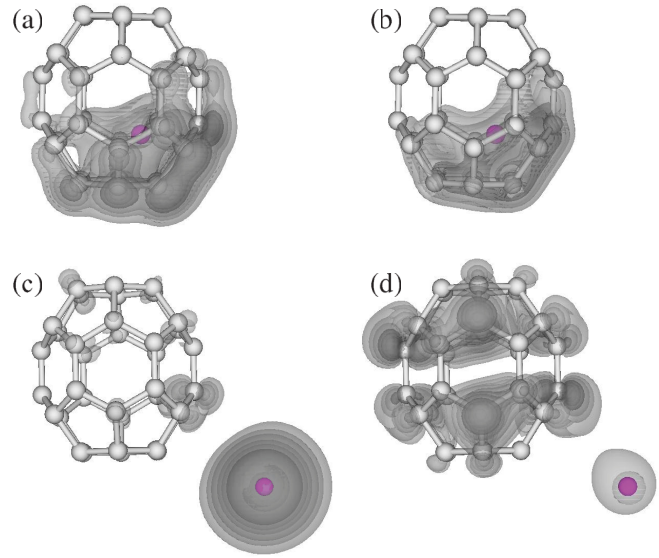

FIG. 8. (Color online) Electron density contributions from the second and the third most important molecular orbitals (the first MO, which is the 1s core atomic orbital of ^{7}Be, is not shown): (a) second MO of ^{7}Be@C_{36}, (b) third MO of ^{7}Be@C_{36}. (c) second MO when ^{7}Be is outside C_{36}, and (d) third MO when ^{7}Be is outside C_{36}.

V. CONCLUSIONS

In summary, using a high-accuracy *ab initio* approach (the Hartree-Fock method with electron correlation treatment according to MP2 or SDCI implemented in our original code [32,33]) we have found equilibrium geometries for the ^{7}Be atom located inside and outside the C_{36} fullerene and predicted an appreciable 2.5% increase of the half-life decay time of the ^{7}Be nucleus in the ^{7}Be@C_{36} molecule in comparison with ^{7}Be@C_{60}. The driving force of the effect is the decrease of the electron density $\rho(0)$ at the ^{7}Be nucleus in ^{7}Be@C_{36} which is caused by the "oxidation" of ^{7}Be by the C_{36} fullerene. If ^{7}Be is located outside C_{36} then the electron density at ^{7}Be is almost the same as in the case of a single ^{7}Be atom. Our theoretical findings for the molecular complex can be checked experimentally since the effect is certainly within the accuracy of modern nuclear measurements.

[1] E. Segre, Phys. Rev. **71**, 274 (1947).
[2] E. Segre and C. E. Wiegand, Phys. Rev. **75**, 39 (1949); **81**, 284(E) (1951).
[3] R. Daudel, Rev. Sci., Paris **85**, 162 (1947).
[4] R. F. Leininger, E. Segre, and C. Wiegand, Phys. Rev. **76**, 897 (1949); **81**, 280(E) (1951).
[5] J. J. Kraushaar, E. D. Wilson, and K. T. Bainbridge, Phys. Rev. **90**, 610 (1953).
[6] H. W. Johlige, D. Aumann, and H.-J. Born, Phys. Rev. C **2**, 1616 (1970).
[7] C.-A. Huh, Earth Planet. Sci. Lett. **171**, 325 (1999).

[8] F. Lagoutine, J. Legrand, and C. Bac, Int. J. Appl. Radiat. Isot. **26**, 131 (1975).
[9] Y. Nir-El *et al*., Phys. Rev. C **75**, 012801(R) (2007).
[10] A. Ray *et al*., Phys. Lett. B **455**, 69 (1999).
[11] E. B. Norman *et al*., Phys. Lett. B **519**, 15 (2001).
[12] Z.-Y. Liu *et al*., Chin. Phys. Lett. **20**, 829 (2003).
[13] A. Ray *et al*., Phys. Rev. C **73**, 034323 (2006).
[14] V. Kumar, M. Hass, Y. Nir-El, G. Haquin, and Z. Yungreiss, Phys. Rev. C **77**, 051304(R) (2008).
[15] B. N. Limata *et al*., Eur. J. Phys. A **27**, Suppl. 1, 193 (2006).
[16] D. J. Souza *et al*., J. Nucl. Sci. Technol. Suppl. **2**, 470 (2002).
[17] T. Ohtsuki, K. Ohno, T. Morisato, T. Mitsugashira, K. Hirose, H. Yuki, and J. Kasagi, Phys. Rev. Lett. **98**, 252501 (2007).
[18] M. Jaeger, S. Wilmes, V. Kolle, G. Staudt, and P. Mohr, Phys. Rev. C **54**, 423 (1996).
[19] T. Ohtsuki, H. Yuki, M. Muto, J. Kasagi, and K. Ohno, Phys. Rev. Lett. **93**, 112501 (2004).
[20] W. K. Hensley, W. A. Basset, and J. R. Huizenga, Science **181**, 1164 (1973).
[21] L.-G. Liu and C.-A. Huh, Earth Planet. Sci. Lett. **180**, 163 (2000).
[22] B. Wang *et al*., Eur. J. Phys. A **28**, 375 (2006).
[23] W. Bambynek *et al*., Rev. Mod. Phys. **49**, 77 (1977).
[24] J. Boruta and K. Makariunas, Phys. Lett. A **71**, 47 (1979).
[25] J. Lu, Y. Zhou, X. Zhang, and X. Zhao, Chem. Phys. Lett. **352**, 8 (2002).
[26] A. Ray, P. Das, S. K. Saha, S. K. Das, and A. Mookerjee, Phys. Rev. C **66**, 012501(R) (2002).
[27] A. Ray, P. Das, S. K. Saha, and S. K. Das, Phys. Lett. B **531**, 187 (2002).
[28] T. Morisato, K. Ohno, T. Ohtsuki, K. Hirose, M. Sluiter, and Y. Kawazoe, Phys. Rev. B **78**, 125416 (2008).
[29] E. V. Tkalya, A. V. Bibikov, and I. V. Bodrenko, Phys. Rev. C **81**, 024610 (2010).
[30] J. C. Grossman *et al*., in *Fullerenes: Chemistry, Physics and Technology*, edited by K. M. Kadish and R. S. Ruoff (Wiley, New York, 2000), p. 887.
[31] A. Szabo and N. Ostlund, *Modern Quantum Chemistry* (McGraw-Hill, Dover, 1989).
[32] A. Artemyev, A. Bibikov, V. Zayets, and I. Bodrenko, J. Chem. Phys. **123**, 024103 (2005).
[33] A. V. Nikolaev, I. V. Bodrenko, and E. V. Tkalya, Phys. Rev. A **77**, 012503 (2008).
[34] T. H. Dunning Jr., J. Chem. Phys. **90**, 1007 (1989).
[35] R. L. Murry and G. E. Scuseria, Science **263**, 791 (1994).